The Canadian Mineralogist
Vol. 49, pp. 1045-1054 (2011)
DOI: 10.3749/canmin.49.4.1045

THE CRYSTAL CHEMISTRY OF LIZARDITE-1*T* FROM NORTHERN APENNINES OPHIOLITES NEAR MODENA, ITALY

ANGELA LAURORA, MARIA FRANCA BRIGATTI§, DANIELE MALFERRARI,
ERMANNO GALLI AND ANTONIO ROSSI

Dipartimento di Scienze della Terra, Università di Modena e Reggio Emilia, Largo S. Eufemia 19, I–41121 Modena, Italy

MASSIMO FERRARI

via Gramsci 285, I–41122 Modena, Italy

ABSTRACT

We investigated the crystal-chemical features of six crystals of lizardite-1*T* sampled in four outcrops of ophiolite, at Pompeano, Sassomorello, Varana, and Santa Scolastica, in the Modena Apennines, Italy. In spite of the extensive contributions already present in the literature, this is the first study dealing with lizardite from the Modena ophiolites. As is clear from one of our samples, the whole-rock composition affects the composition of lizardite, which makes it susceptible to overprinting by later metasomatic events. In our study, we paid particular attention to the effects of $^{VI}Mg_{-1}{}^{VI}Fe^{2+}$ and of $^{IV}Si_{-1}{}^{IV}Al{}^{VI}(Mg, Mn, Fe)^{2+}{}_{-1}{}^{VI}(Al, Cr, Fe)^{3+}$ exchange mechanisms on the structure. Our results suggest that $^{VI}Mg_{-1}{}^{VI}Fe^{2+}$ substitution induces an increase in the *M*–O4 length in octahedra and a decrease in the octahedral-site distortion. Both these effects are also observed to influence the unit-cell parameter *c*. The effect of the $^{IV}Si_{-1}{}^{IV}Al{}^{VI}(Mg, Mn, Fe)^{2+}{}_{-1}{}^{VI}(Al, Cr, Fe)^{3+}$ substitution is to decrease the *M*–O1 distance and concomitantly, to increase the *T*–O1 distance.

Keywords: lizardite, ophiolite, crystal chemistry, exchange mechanisms, metasomatism, northern Appenines, Italy.

SOMMAIRE

Nous avons étudié les aspects cristallochimiques de six cristaux de lizardite-1*T* prélevés sur quatre affleurements d'ophiolite, situés à Pompeano, Sassomorello, Varana, et Santa Scolastica, dans les Appenins de la région de Modena, en Italie. Malgré les contributions volumineuses déjà dans la littérature, nous présentons les premiers résultats portant sur la lizardite des ophiolites de la région de Modena. Il est clair dans un de nos échantillons que la composition globale de la roche influence la composition de la lizardite, ce qui la rend susceptible à changer lors des événements de métasomatose ultérieurs. Dans notre travail, nous avons porté une attention toute particulière aux effets structuraux des substitutions d'échange $^{VI}Mg_{-1}{}^{VI}Fe^{2+}$ et $^{IV}Si_{-1}{}^{IV}Al{}^{VI}(Mg, Mn, Fe)^{2+}{}_{-1}{}^{VI}(Al, Cr, Fe)^{3+}$. D'après nos résultats, la substitution $^{VI}Mg_{-1}{}^{VI}Fe^{2+}$ cause une augmentation de la longueur *M*–O4 dans les octaèdres et une diminution dans la distorsion du site octaédrique. Ces deux facteurs influencent le paramètre réticulaire *c*. La substitution $^{IV}Si_{-1}{}^{IV}Al{}^{VI}(Mg, Mn, Fe)^{2+}{}_{-1}{}^{VI}(Al, Cr, Fe)^{3+}$ cause une diminution de la distance *M*–O1 et une augmentation concomitante de la distance *T*–O1.

(Traduit par la Rédaction)

Mots-clés: lizardite, ophiolite, cristallochimie, mécanismes d'échange, métasomatose, chaîne des Appenins, Italie.

INTRODUCTION

In this paper, we investigate the crystal-chemical and structural features of six crystals of lizardite sampled in the ophiolitic outcrops at Pompeano, Sassomorello, Varana, and Santa Scolastica, in the Modena sector of the northern Apennines, Italy. We also aim, where possible, to establish a relationship between the crystal chemistry of the mineral and its genetic environment. This is the first study of lizardite from the area of the Modena ophiolites. The bodies of ophiolite (359 outcrops encompassing serpentinites, gabbros, diabases, breccias, and hydrothermally affected rocks) in fact have barely been investigated; petrographic and petro-

§ *E-mail address*: brigatti@unimore.it

logical outlines are given in some papers (Bertolani *et al.* 1963, Bertolani & Capedri 1966, Capedri *et al.* 1979, Capedri & Toscani 2000), but deserve more intense study. Further chemical and mineralogical information is occasionally reported in papers dealing with the general role of ophiolites in the Mediterranean basin (*e.g.*, Dostal *et al.* 1975, 1977, Capedri & Venturelli 1979, 1988).

Background Information

Lizardite, which commonly is present in ophiolites, is a 1:1 trioctahedral phyllosilicate with the general formula $Mg_3Si_2O_5(OH)_4$, composed of alternating sheets of octahedra and tetrahedra (Wicks & Whittaker 1975, Wicks & O'Hanley 1988). It is the flat-layer serpentine polymorph, the other two being antigorite and chrysotile, the first one characterized by periodic reversals of layer polarity, and the second one by cylindrically rolled layers. For each of these three phases, polytypism, polysomatism, and chemical variability account for a great structural unpredictability (Hilairet *et al.* 2006). Examples of complex variations in serpentine structure are the so-called polygonal and polyhedral serpentines. Polygonal serpentines consist of fibers each showing 15 or 30 arranged sectors (Baronnet & Devouard 2005); polyhedral serpentines consist of spheroids of 92 or 176 lizardite crystals, each one defining a triangular, and in the case of the large spheres, hexagonal facet of the spheroid (Baronnet *et al.* 2007, Cressey *et al.* 2010). Antigorite is inferred to be more stable at high pressure and high temperature (HP–HT) conditions (Mellini & Zanazzi 1989), thus accounting for its presence in rocks showing high-pressure assemblages of minerals (Wunder & Schreyer 1997). The factors leading to the occurrence of such structural varieties as lizardite and chrysotile, instead of antigorite, are still poorly defined, and the relative fields of stability of these phases are not yet quantitatively constrained. Furthermore, direct observations are very difficult because of the common intergrowth of structural varieties. Some authors have suggested that the appearance of lizardite or chrysotile is related to the environment of crystallization and to kinetic factors rather than to P–T conditions only, and that chrysotile is a metastable phase (Evans 2004). Andreani *et al.* (2008) argued that polyhedral serpentine is generated during the last stages of serpentine crystallization, *i.e.*, in the lower part of the field of serpentine stability, which is only constrained by $T < 600°C$ (Evans 2004). The same authors also proposed that not only polyhedral serpentine, but also other serpentines, such as chrysotile, could crystallize from a protoserpentine, which would represent the first step in the structural organization of a gel.

Extensive X-ray, neutron diffraction, and TEM studies are available for lizardite from Monte Fico quarries, Elba Island, Italy (Mellini & Viti 1994, Viti & Mellini 1997, Gregorkiewitz *et al.* 1996), Val Sissone, Italy (Mellini 1982), and Monte Tre Abati, Coli, Italy (Mellini & Zanazzi 1987). Experimental studies were also carried out on lizardite from these occurrences under high-temperature (Guggenheim & Zhan 1998) and high-pressure (Mellini & Zanazzi 1989) conditions, in order to assess structural variations induced on the mineral. In a very recent study, Mellini *et al.* (2010) described the crystal structure of a Mg end-member lizardite-1*T* from polyhedral spheres of serpentine at the Lizard, Cornwall.

Geological Setting, Sample Occurrence and Description

All our lizardite crystals were sampled from thin veins or crusts present on the surfaces of ophiolite outcrops. The Pompeano ophiolite (596 m.a.s.l.; 44°23'54.46"N, 10°45'25.54"E) is a serpentinite located in the middle of the Rossenna River valley, not far from the town of Serramazzoni; it crops out in the surrounding countryside, which is composed of Palombini Clays (Fig. 1a). Lizardite from Pompeano comes in two varieties, the first one being represented by fibrous crystals, and the second one by massive trigonal prisms. We were able to refine and discuss only the latter. Trigonal prisms range in color from dark to light green, and are present in the matrix of bulk serpentine (Ferrari 1994).

The Sassomorello and Varana serpentinites resemble each other, and also show similar structures and compositions with the Pompeano serpentinite. The Sassomorello outcrop (650 m of maximum extent; 44°25'27.36"N, 10°44'17.17"E) is located close to the village of Sassomorello along the Rossenna River, in the district of Serramazzoni. It is delimited by straight escarpments and crops out in the surrounding landscape composed of Palombini Clays (Fig. 1a). The outcrop consists of breccias with serpentinite clasts of variable dimensions. Locally, gabbroic clasts also are present. The Varana outcrop (650 m of maximum extent; 44°27'20.66"N, 10°46'28.73"E) is located close to the village of Varana along the Fossa River, also in the district of Serramazzoni. It presents steep escarpments that overlie the surrounding Palombini Clays (Fig. 1a). It consists of two rock clusters, leveled on the top, and of a detrital cluster of boulders made of large fragments. The first cluster is 5–6 m high; the second one is up to 10–12 m high. At both Sassomorello and Varana, the lizardite occurs as trigonal prisms.

The S. Scolastica outcrop (<100 m in diameter; 44°19'13.00"N, 10°32'08.26"E) is located in the Dolo Valley, next to Romanoro, a village in the district of Frassinoro (Fig. 1b). It is quite different from the previously described outcrops because it bears the signs of interaction of the former peridotite with a metasomatic fluid rich in Ca, Fe, Ti, and Mn, possibly related to the serpentinization event (Capedri & Lugli 1999). Minor phases formed during fluid–rock interaction are in the

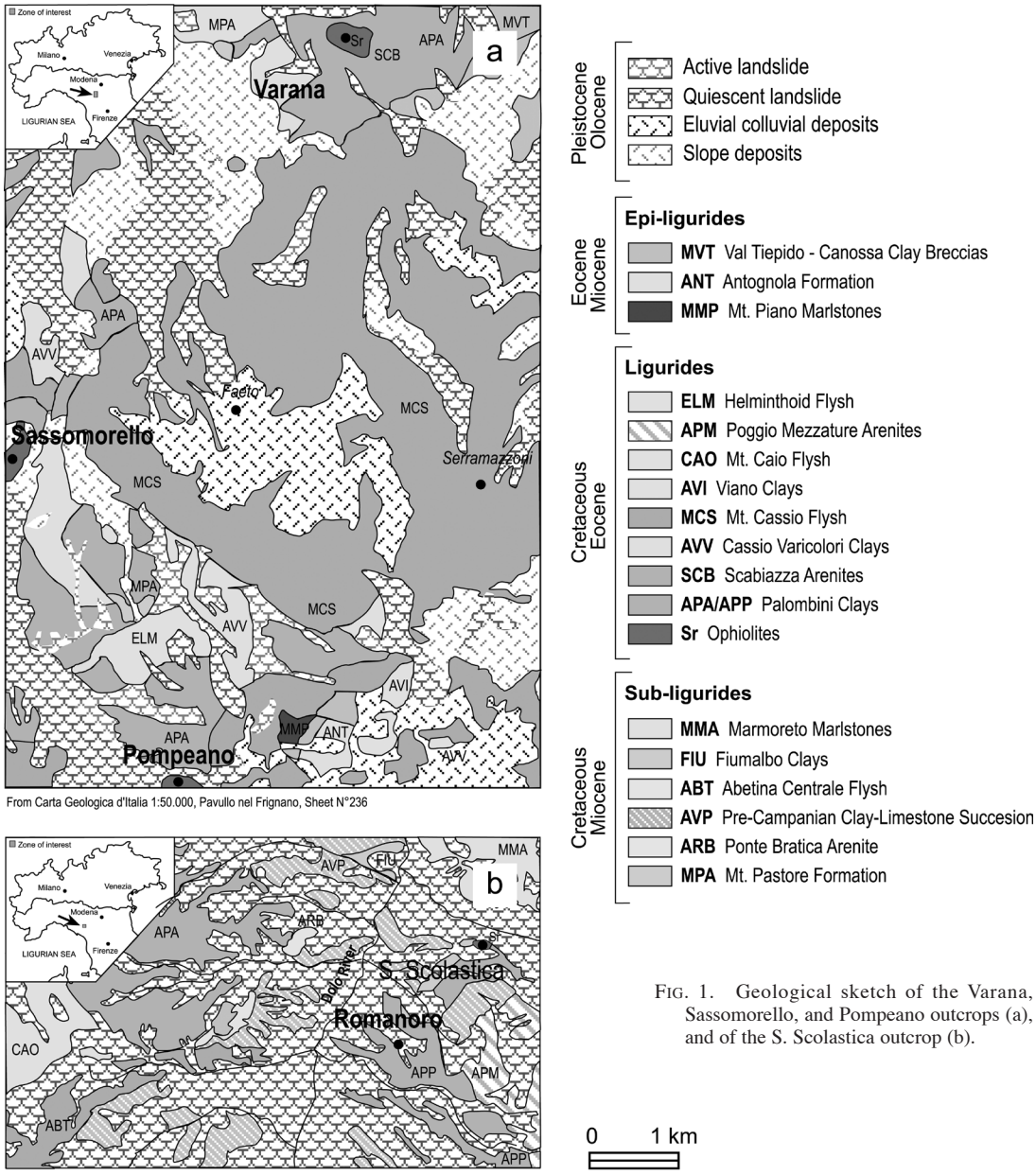

FIG. 1. Geological sketch of the Varana, Sassomorello, and Pompeano outcrops (a), and of the S. Scolastica outcrop (b).

form of aggregates of oxides of the ilmenite–pyrophanite series ($Fe^{2+}TiO_3$–$Mn^{2+}TiO_3$), which are absent in the other serpentinites. Grains of sulfides of Ni–Fe a few micrometers in size also are present. Lizardite from S. Scolastica is found either as trigonal prisms, or as characteristic aggregates with a six-cornered star shape, never before described in literature (Figs. 2a, b). Only trigonal prisms were found to be suitable for X-ray diffraction and refinement. The star-shaped crystals, up to 100 μm in size, were studied with SEM–EDS (Philips XL–30 equipped with a Oxford INCA–350), and a Gandolfi camera. The analyses performed, though they confirm the structural and chemical features of the samples (*i.e.*, they all are lizardite), seem to exclude any similarity of these crystals with either polyhedral or polygonal serpentines.

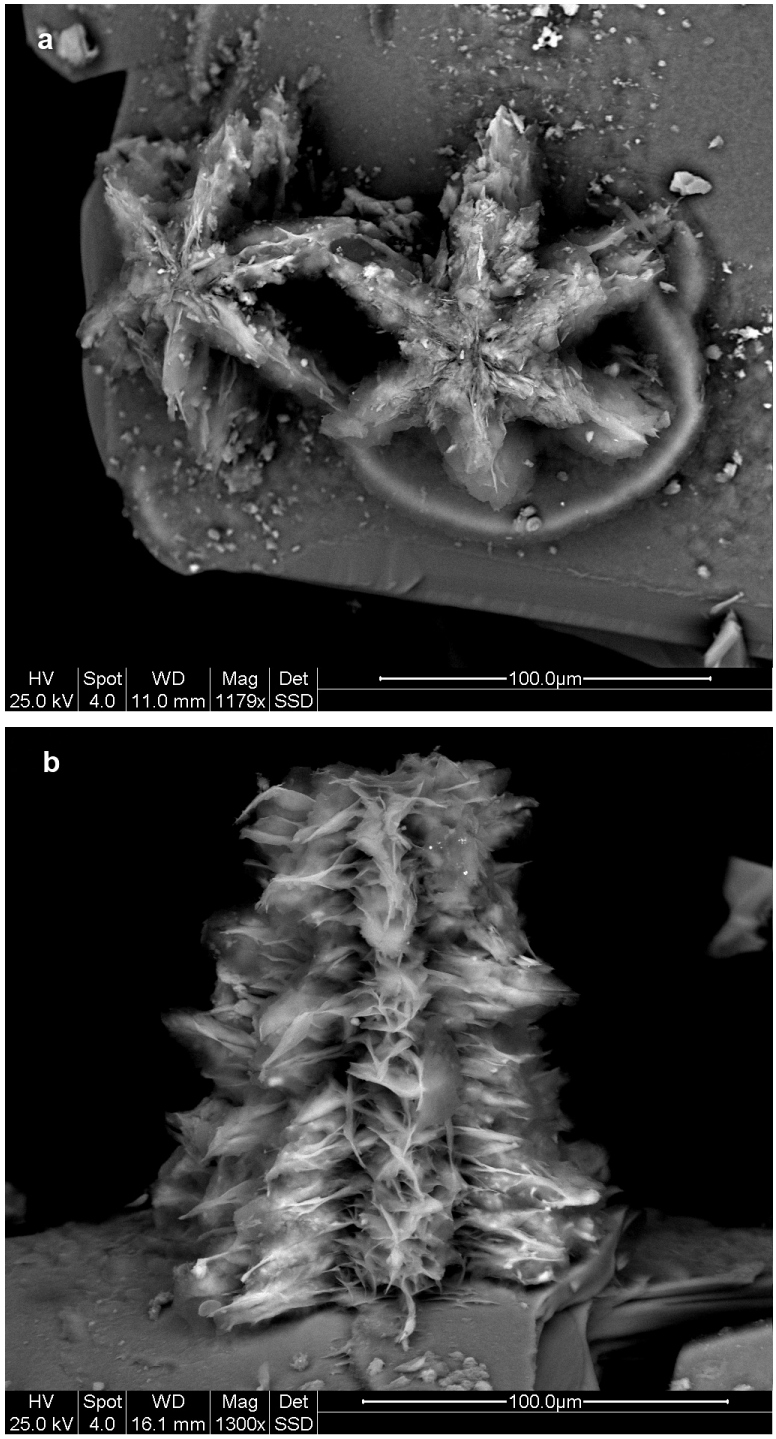

FIG. 2. SEM secondary electron images (a, b) of the characteristic aggregates of lizardite crystals with a six-cornered star shape.

Chemical Composition and Chemical Formulae

Chemical analyses were carried out with an ALR–SEMQ microprobe with four WDS spectrometers on ten samples, including those used for X-ray diffraction (see Table 1, and next paragraph). The crystals of lizardite show $Fe^{2+}/(Fe^{2+} + Mg)$ values varying from 0.04 [Pompeano (3)] to 0.12 [S. Scolastica (1)]. In agreement with the hypothesis of a Fe-bearing metasomatic fluid affecting the serpentinite outcrop of S. Scolastica (Capedri & Lugli 1999), the lizardite of S. Scolastica (1) shows the highest value of that ratio.

Calculations of the chemical formulae and structure refinements suggest that, at least in the case of samples Pompeano (4) and Varana (1), part of the Fe content could be in its oxidized form. The Al_{tot} content varies from 0.03 [Pompeano (1)] to 0.24 atoms per formula unit (*apfu*) [Varana (2)]. The Al_{tot} contents of the Varana crystals are similar to the value of lizardite from Val Sissone (Mellini 1982), which was the highest ever measured in a refined crystal. Other samples of lizardite refined so far show lower Al contents (Mellini & Zanazzi 1987, Mellini & Viti 1994, Hilairet *et al*. 2006). The Pompeano crystals are characterized by a remarkable variability, with Al_{tot} values from 0.03 [Pompeano (1)] to 0.21 *apfu* [Pompeano (3)]. The S. Scolastica crystals also show a significant variability [0.13–0.20 *apfu* for S. Scolastica (2) and (1), respectively].

The ^{VI}Al content of our samples is strictly related to Al_{tot}, the sample Pompeano (1) showing the lowest value and the sample Varana (2) the highest one. With the exception of Pompeano (1), Pompeano (4), and Santa Scolastica (2) and (3), our samples are richer in ^{VI}Al than lizardite from Val Sissone, which is characterized by a noticeably low Si content (1.830 *apfu*).

Crystal-Structure Refinements

It is well known that the crystal structure of lizardite is formed by a stacking of 1:1 layers, each one containing a pseudohexagonal sheet of corner-shared SiO_4 units linked to a trioctahedral sheet of edge-

TABLE 1. CHEMICAL COMPOSITION AND FORMULA OF LIZARDITE CRYSTALS

Sample	Pompeano				Sasso-morello	Varana		Santa Scolastica		
n	(1)* 6	(2) 6	(3)* 6	(4)* 8	* 6	(1)* 8	(2)* 6	(1)* 8	(2) 6	(3) 6
SiO_2 wt%	42.82 0.67	42.06 0.16	40.53 0.51	40.52 0.28	40.87 0.18	39.99 0.21	40.07 0.64	39.46 0.34	41.44 0.64	40.48 0.32
Al_2O_3	0.50 0.11	2.15 0.11	3.80 0.18	3.27 0.14	2.71 0.10	4.04 0.17	4.25 0.33	3.53 0.16	2.35 0.15	2.53 0.09
Cr_2O_3	0.02 0.01	0.00	0.01 0.01	0.00	0.03 0.02	0.00	0.01 0.01	0.01 0.01		0.01 0.01
Fe_2O_3				1.45		0.03				0.38
FeO	7.38 0.95	5.21 0.19	2.72 0.07	4.86 0.11	4.47 0.29	3.59 0.16	3.71 0.11	8.42 0.17	3.79 0.16	4.20 0.12
MnO	0.14 0.03	0.04 0.02	0.03 0.01	0.06 0.01	0.06 0.01	0.06 0.02	0.05 0.02	0.24 0.01	0.04 0.02	0.06 0.01
MgO	38.97 1.01	39.23 0.42	39.95 0.48	38.84 0.67	39.12 0.25	39.99 0.85	39.05 0.52	35.40 0.26	39.98 0.79	38.88 0.34
Sum	89.83	88.69	87.04 0.53	88.99	87.26	86.70	87.14	87.06	87.60	86.54
$^{[IV]}$Si *apfu*	1.989	1.952	1.896	1.885	1.924	1.887	1.882	1.903	1.936	1.922
$^{[IV]}$Al	0.011	0.048	0.104	0.115	0.076	0.113	0.118	0.097	0.064	0.078
Sum	2.000	2.000	2.000	2.000	2.000	2.000	2.000	2.000	2.000	2.000
$^{[VI]}$Al	0.016	0.070	0.106	0.064	0.074	0.112	0.117	0.104	0.065	0.064
$^{[VI]}Cr^{3+}$	0.001	0.000	0.000	0.000	0.001	0.000	0.000	0.000	0.000	0.000
$^{[VI]}Fe^{3+}$	0.000	0.000	0.000	0.051	0.000	0.001	0.000	0.000	0.000	0.013
$^{[VI]}Fe^{2+}$	0.286	0.202	0.106	0.189	0.176	0.142	0.146	0.340	0.148	0.167
$^{[VI]}Mn^{2+}$	0.005	0.002	0.001	0.002	0.002	0.002	0.002	0.010	0.002	0.003
$^{[VI]}Mg^{2+}$	2.690	2.715	2.786	2.694	2.746	2.743	2.734	2.545	2.784	2.753
Sum	2.998	2.989	2.999	3.000	2.999	3.000	2.999	2.999	2.999	3.000
Mg#	0.904	0.931	0.963	0.918	0.940	0.950	0.949	0.882	0.950	0.939
Mean Electron Count										
M(XREF)§			12.9(2)	13.3(2)	13.5(1)	13.0(2)	13.1(1)	13.7(2)		
M(EPMA)¶	13.4	12.9	12.5	13.2	12.9	12.7	12.7	13.7	12.7	12.87

Note: (*) used in single-crystal X-ray diffraction study; Mg# = Mg / (Mg + Fe_{tot}); XREF: single-crystal X-ray refinement; EPMA: electron-probe microanalysis. The unit-cell content is recalculated on the basis of $O5(OH)_4$. *n*: number of point analyses.

sharing $MgO_2(OH)_4$ octahedra. For more details, see Figures 2 and 3 in Mellini (1982). Single-crystal X-ray diffraction data were collected using a Bruker X8–Apex fully automated four-circle diffractometer with Kappa geometry, ceramic X-ray tube KFF–Mo–2k–90 Fine Focus and APEX 4K CCD area detector. The crystal structure was refined using the SHELX–97 package of programs (Sheldrick 1997) starting from the atom coordinates of Mellini (1982). Successive refinements were performed on six selected lizardite crystals: Pompeano (3), Pompeano (4), Sassomorello, Varana (1), Varana (2), and S. Scolastica (1). An idealized chemical composition was assumed for most cycles in the refinement; the last one included data on the chemical composition derived from the electron-microprobe analyses. This approach allowed us to derive Fe, Mg partition in octahedral sites. During final refinement loop, H atoms were determined by Fourier-difference synthesis. The coordinates of hydrogen atoms were fixed when O–H distances consistent with literature evidence were attained. To minimize correlation effects, the isotropic U values of both symmetrically independent H atoms were assumed to vary commonly. For each sample, the number of collected and unique reflections, the internal and final *R* values, the goodness of fit, the explored θ range, and the completeness parameter are reported in Table 2. Relevant bond-lengths and the α parameter are reported in Table 3, whereas coordinates and isotropic and anisotropic displacement factors of atoms are available from the Depository of Unpublished Data on the on the Mineralogical Association of Canada website [document Lizardite CM49_1045]. The nomenclature of sites in this paper follows the convention: *T*: tetrahedral cations, *M*: octahedral cations, O1: apical tetrahedron oxygen atom, O2: basal tetrahedron oxygen atoms, O3: outer octahedron hydroxyl groups, O4: inner octahedron hydroxyl groups. The *R* final values [R_F (%)] range from 3.21 [Varana (2)] to 3.99 [Varana (1)]. All the examined samples of lizardite crystallize in space group *P*31*m* and belong to the 1*T* polytype. Their *a* and *c* unit-cell parameters vary from 5.3230(8) (Sassomorello) to 5.3263(4) Å [Santa Scolastica (1)] and from 7.2680(1) [Pompeano (4)] to 7.2885(7) Å [S. Scolastica (1)], respectively (Table 2). Their α parameter ranges from –2.38° [S.Scolastica (1)] to –2.82° [Varana (2)]. In general, the observed structural parameters well agree with previous observations on lizardite-1*T* made by Mellini (1982) and Mellini & Viti (1994).

Discussion

The crystal structure of lizardite is well established in the literature, both at ambient conditions and varying temperature and pressure conditions (Guggenheim & Zhan 1998, Gregorkiewitz *et al.* 1996, Hilairet *et al.* 2006, Mellini & Zanazzi 1989). Less attention has been directed to the geometrical modifications induced by chemical substitutions, because the main exchange-vectors [*e.g.*, $^{VI}Mg_{-1}{}^{VI}Fe^{2+}$ and $^{IV}Si_{-1}{}^{IV}Al{}^{VI}(Mg, Mn, Fe)^{2+}{}_{-1}{}^{VI}(Al, Cr, Fe)^{3+}$] appear to be limited in the 1*T* polytype, and the structural variability seems to be limited as well.

The effect of the homovalent $^{VI}Mg_{-1}{}^{VI}Fe^{2+}$ substitution is shown in Figure 3a, where the *M*–O4 distance, *i.e.*, the distance between the octahedrally coordinated cations and the inner hydroxyl groups, increases with the $Fe^{2+}/(Fe^{2+} + Mg)$ value. In this figure and in the following ones, data from Mellini & Viti (1994), Mellini (1982), Mellini & Zanazzi (1987), and Guggenheim & Zhan (1998) are plotted for comparison. The $^{VI}Mg_{-1}{}^{VI}Fe^{2+}$ substitution also produces a decrease in the distortion of the octahedral site (calculated as maximum octahedron edge minus minimum octahedron edge, all divided by mean octahedron edge), due to the shortening of the longest unshared octahedron edge and to the lengthening of the shortest one (Fig. 3b). This effect is also evident in Figure 3c, where the difference between shared and unshared edges is plotted against the mean *M*–O length in the octahedra. It appears, in fact, that where the dimension of the octahedral site increases, the octahedron becomes more regular.

The geometrical variation of the octahedron influences the entire structure, as the unit-cell parameter *c* is related to the difference between shared and unshared edges of the octahedra, and the unit-cell parameter *a* mostly depends upon the unshared edges (Figs. 4a, 4b).

TABLE 2. UNIT-CELL PARAMETERS OF LIZARDITE-1*T* CRYSTALS AND INFORMATION RELATED TO X-RAY DATA COLLECTION

Sample	N collected	N unique	R_{int} %	R_F %	Goodness of fit	θ_{min} °	θ_{max} °	Completeness, %	*a* Å	*c* Å	*V* Å^3
Pompeano (3)	1534	496	1.84	3.92	1.156	4.42	34.15	94.90	5.3234(2)	7.2721(4)	178.47(1)
Pompeano (4)	1717	536	2.25	3.91	1.057	4.42	34.41	93.40	5.3244(6)	7.268(1)	178.43(4)
Sassomorello	4136	1143	2.60	3.85	1.001	2.80	49.55	95.70	5.3230(8)	7.270(2)	178.39(5)
Varana (1)	1763	567	3.35	3.99	1.044	4.42	35.29	96.20	5.3259(1)	7.2726(3)	178.651(9)
Varana (2)	907	382	1.36	3.21	1.160	2.80	32.41	90.90	5.3261(5)	7.273(1)	178.67(3)
Santa Scolastica (1)	1295	451	3.06	3.96	1.051	4.42	31.90	96.40	5.3263(4)	7.2885(7)	179.07(3)

TABLE 3. RELEVANT BOND-LENGTHS OF REFINED LIZARDITE-1*T* CRYSTALS*

Sample	Pompeano (3)	Pompeano (4)	Sassomorello	Varana (1)	Varana (2)	Santa Scolastica (1)
Tetrahedron (*T*)						
T – O1	1.593(4)	1.594(5)	1.601(2)	1.600(4)	1.596(4)	1.592(5)
T – O2 (× 3)	1.649(1)	1.651(2)	1.6460(5)	1.650(1)	1.654(2)	1.650(5)
⟨*T* – O⟩	1.635	1.637	1.635	1.638	1.640	1.636
Tetrahedron edges						
O1 – O2 (× 3)	2.676(4)	2.681(5)	2.675(2)	2.681(4)	2.688(5)	2.675(7)
O2 – O2 (× 3)	2.6624(2)	2.6629(3)	2.6622(4)	2.6636(1)	2.6639(3)	2.6637(3)
⟨O – O⟩	2.669	2.672	2.669	2.672	2.676	2.669
Ring of tetrahedra: distortion						
α (°)	–2.58	–2.54	–2.66	–2.62	–2.82	–2.38
Octahedron (*M*)						
M – O3	2.018(2)	2.015(3)	2.022(1)	2.023(2)	2.011(2)	2.022(3)
M – O3 (× 2)	2.018(1)	2.014(3)	2.022(1)	2.024(2)	2.012(2)	2.023(3)
M – O4	2.097(3)	2.105(3)	2.096(1)	2.098(3)	2.098(3)	2.106(5)
M – O1 (× 2)	2.132(2)	2.135(3)	2.130(1)	2.131(2)	2.133(2)	2.136(4)
⟨*M* – O⟩	2.069	2.070	2.070	2.072	2.067	2.074
Octahedron edges: unshared						
O3 – O3 (× 2)	3.069(2)	3.071(2)	3.0688(8)	3.070(2)	3.070(2)	3.070(4)
O3 – O3	3.083(4)	3.081(5)	3.082(2)	3.084(4)	3.086(4)	3.085(6)
O1 – O1	3.0735(1)	1 3.0740(4)	3.0732(5)	3.075(1)	3.0750(3)	3.0751(2)
O1 – O4 (× 2)	3.0739(1)	3.0744(4)	3.0737(5)	3.075(1)	3.0755(3)	3.075(1)
$\langle O - O \rangle_{unsh}$	3.074	3.074	3.073	3.075	3.075	3.075
Octahedron edges: shared						
O3 – O4 (× 2)	2.743(5)	2.745(5)	2.747(2)	2.750(3)	2.731(5)	2.759(7)
O3 – O1 (× 2)	2.778(4)	2.776(4)	2.781(2)	2.783(4)	2.766(4)	2.788(5)
O3 – O1 (× 2)	2.778(4)	2.776(4)	2.781(2)	2.783(4)	2.766(4)	2.788(6)
$\langle O - O \rangle_{sh}$	2.766	2.760	2.770	2.772	2.754	2.778
Hydrogen – oxygen bonds						
O3 – H3	0.998(3)	0.958(3)	1.034(1)	1.018(3)	1.076(2)	0.978(5)
O4 – H4	1.083(5)	1.014(5)	1.050(2)	1.045(5)	0.984(3)	1.091(7)

Note: α (angle of tetrahedron rotation) = $\sum_{i=1}^{6} \alpha_i / 6$, where $\alpha_i = |120° - \varphi_i|/2$, and where φ_i is the angle between basal edges of neighboring tetrahedra articulated in the ring.

The mineral structure is also influenced by the exchange vector $^{IV}Si_{-1}\ ^{IV}Al\ ^{VI}(Mg, Mn, Fe)^{2+}_{-1}\ ^{VI}(Al, Cr, Fe)^{3+}$, which induces a decrease in the *M*–O1 distance and an increase in the *T*–O1 distance (Table 3).

The trend that characterizes our samples and samples from literature plotted for comparison (Figs. 3, 4), *i.e.*, a direct correlation between the mean *M*–O distance in octahedra, the regularity of the octahedron, and the unit-cell parameter *c*, is also observed in data obtained by Guggenheim & Zhan (1998) on a lizardite-1*T* crystal from Val Sissone at increasing values of temperature. The idea of gaining information about temperature conditions during crystallization by studying geometrical modifications of octahedra in lizardite is very attractive; unfortunately, on the basis of our results, octahedron regularity depends not only on temperature but also on chemical composition (*i.e.*, $^{VI}Mg_{-1}\ ^{VI}Fe^{2+}$ substitution). Furthermore, whereas some authors argued that equilibrium rather than kinetic factors affects the development of serpentine mineralogy (O'Hanley *et al.* 1989), others stated that kinetic factors are quite relevant during lizardite crystallization (Evans 2004).

From previous studies, there is no evidence of a dependence between temperature and $^{VI}Mg_{-1}\ ^{VI}Fe^{2+}$ substitution during lizardite crystallization. However,

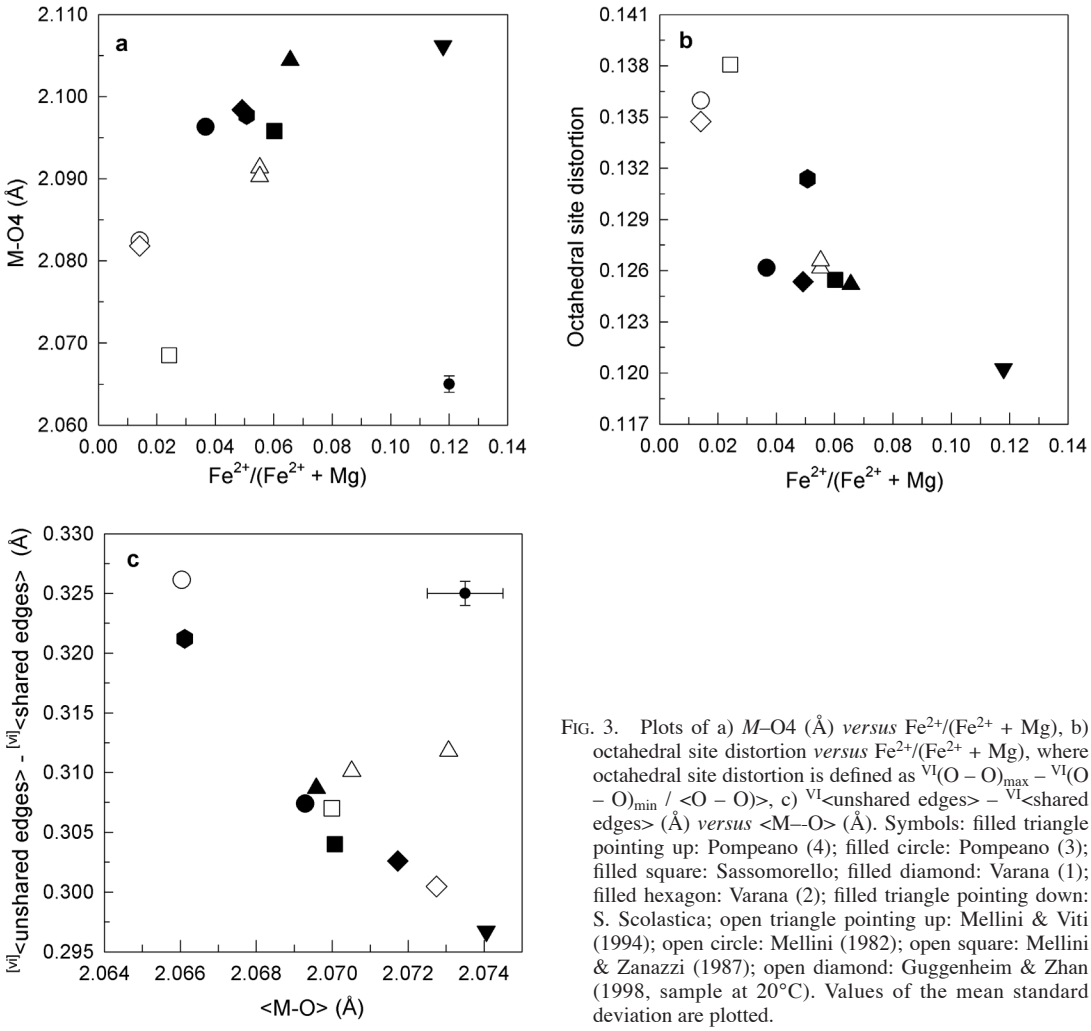

FIG. 3. Plots of a) *M*–O4 (Å) *versus* $Fe^{2+}/(Fe^{2+} + Mg)$, b) octahedral site distortion *versus* $Fe^{2+}/(Fe^{2+} + Mg)$, where octahedral site distortion is defined as $^{VI}(O - O)_{max} - {}^{VI}(O - O)_{min}$ / <O – O)>, c) ^{VI}<unshared edges> – ^{VI}<shared edges> (Å) *versus* <M–O> (Å). Symbols: filled triangle pointing up: Pompeano (4); filled circle: Pompeano (3); filled square: Sassomorello; filled diamond: Varana (1); filled hexagon: Varana (2); filled triangle pointing down: S. Scolastica; open triangle pointing up: Mellini & Viti (1994); open circle: Mellini (1982); open square: Mellini & Zanazzi (1987); open diamond: Guggenheim & Zhan (1998, sample at 20°C). Values of the mean standard deviation are plotted.

we suggest a concurrence of these two parameters at least in one of our samples. As described above, sample S. Scolastica (1) shows the highest $Fe^{2+}/(Fe^{2+} + Mg)$ value, the lowest distortion of the octahedral site, as well as of the ring of tetrahedra (*i.e.*, the α parameter). As it comes from a sample of Fe-metasomatized ophiolite (Capedri & Lugli 1999), we argue that the variation induced by the percolating Fe-bearing metasomatic agent, in both bulk-rock composition and temperature, could have affected the structural features of the crystallizing lizardite, evidently without leading to a variation of the 1*T* polytypic sequence.

CONCLUDING REMARKS

In this paper, we examine the crystal-chemical features of lizardite from ophiolite outcrops at Pompeano, Sassomorello, Varana, and S. Scolastica in the Modena Apennines. Our results can be summarized as follows.

1) As evidenced by sample S. Scolastica (1), the whole-rock composition affects the crystal chemistry of lizardite and some structural parameters (*e.g.*, the distortion of the octahedral site and the α parameter), which are susceptible to readjustment owing to secondary, metasomatic events.

2) The chemical composition and structural features of our sample match well the data in the literature (Mellini & Viti 1994, Mellini 1982, Mellini & Zanazzi 1987, Guggenheim & Zhan 1998, their sample at 20°C).

3) The homovalent $^{VI}Mg_{-1}{}^{VI}Fe^{2+}$ substitution produces an increase in the *M*–O4 bond distance, and a decrease in the distortion of the octahedral site.

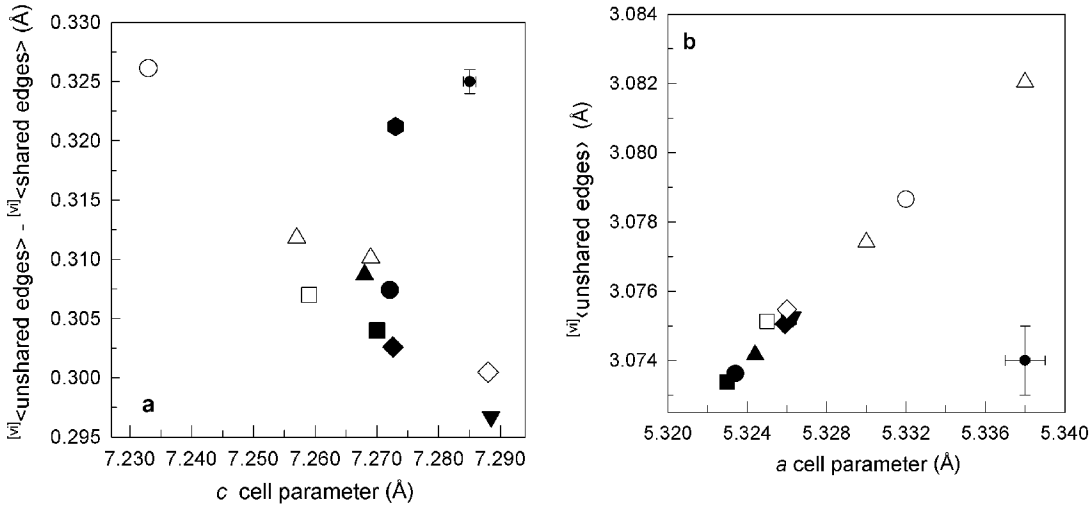

FIG. 4. Plots of (a) ^{VI}<shared edges> – ^{VI}<unshared edges> *versus* unit-cell parameter *c* (Å); (b) ^{VI}<unshared edges> (Å) *versus* unit-cell parameter *a* (Å). Symbols as in Figure 3. Values of the mean standard deviation are plotted.

4) Where the dimension of the octahedral site increases, the octahedron becomes more regular and induces an increase in the unit-cell parameter *c*.

5) The increase in trivalent cations produces a decrease in the *M*–O1 distance and a concomitant increase in the *T*–O1 distance.

ACKNOWLEDGEMENTS

We acknowledge the valuable support of the Editor, Robert F. Martin, Associate Editor Marcello Mellini, and of Fred J. Wicks, an anonymous reviewer and Technical Editor Ron Peterson. Centro Interdipartimentale Grandi Strumenti (CIGS) is also acknowledged for assistance during the analysis of the samples. This work was made possible by the financial support of Ministero dell'Università e della Ricerca Scientifica Project (MIUR PRIN2008) and by the International Project "The relationships of bulk structure. Surface structure, chemistry, and physical properties of mineral phases with six-membered silicate rings" assigned by Fondazione Cassa di Risparmio di Modena.

REFERENCES

ANDREANI, M., GRAUBY, O., BARONNET, A. & MUÑOZ, M. (2008): Occurrence, composition and growth of polyhedral serpentine. *Eur. J. Mineral.* **20**, 159-171.

BARONNET, A., ANDREANI, M., GRAUBY, O., DEVOUARD, B., NITSCHE, S. & CHAUDANSON, D. (2007): Onion morphology and microstructure of polyhedral serpentine. *Am. Mineral.* **92**, 687-690.

BARONNET, A. & DEVOUARD, B. (2005): Microstructures of common polygonal serpentines from axial HRTEM imaging, electron diffraction, and lattice-simulation data. *Can. Mineral.* **43**, 513-542.

BERTOLANI, M. & CAPEDRI, S. (1966): Le ofioliti nelle province di Modena e Reggio Emilia. *Atti della Soc Naturalisti e Matematici di Modena* **47**, 121-170.

BERTOLANI, M., CAPEDRI, S. & LIGABUE, G. (1963): Le ofioliti della valle dello Scoltenna (Appennino Modenese). *Soc. Geol. It., Mem.* **4**, 305-337.

CAPEDRI, S., DE NEGRI, G. & VENTURELLI, G. (1979): Clinopyroxenes and amphiboles in a metadolerite from the northern Apennines. Implications on the palaeogeographic role of ophiolites. *Tschermaks Mineral. Petrogr. Mitt.* **26**, 21-37.

CAPEDRI, S. & LUGLI, S. (1999): Le ofioliti (schede 109-124). *In* I Beni Geologici della Provincia di Modena. Artioli Editore, Modena, Italy.

CAPEDRI, S. & TOSCANI, L. (2000): Subduction-related (?) ophiolitic metabasalts from northern Apennines (Modena Province, Italy). *Chem. Erde* **60**, 111-128.

CAPEDRI, S. & VENTURELLI, G. (1979): Clinopyroxene composition of ophiolitic metabasalts in the Mediterranean area. *Earth Planet. Sci. Lett.* **43**, 61-73.

CAPEDRI, S. & VENTURELLI, G. (1988): Uranium in clinopyroxenes of ophiolitic metabasalts from the Mediterranean area. *Mineral. Petrol.* **38**, 285-289.

CRESSEY, G., CRESSEY, B.A., WICKS, F.J. & YADA, K. (2010): A disc with five-fold symmetry: the proposed fundamental

seed structure for the formation of chrysotile asbestos fibres, polygonal serpentine fibres and polyhedral lizardite spheres. *Mineral. Mag.* **74**, 29-37.

DOSTAL, J., CAPEDRI, S. & AUMENTO, F. (1975): Uranium as an indicator of the origin of the Tethyan ophiolites. *Earth Planet. Sci. Lett.* **26**, 345-352.

DOSTAL, J., DUPUY, C. & CAPEDRI, S. (1977): K, U, Li abundances in ultramafic rocks of Tethyan ophiolites. *Tschermaks Mineral. Petrogr. Mitt.* **24**, 161-168.

EVANS, B.W. (2004): The serpentinite multisystem revisited: chrysotile is metastable. *Int. Geol. Rev.* **46**, 479-506.

FERRARI, M. (1994): La lizardite cristallizzata dell'Appennino Modenese. *Riv. Mineral. It.* **4**, 351-352.

GREGORKIEWITZ, M., LEBECH, B., MELLINI, M. & VITI, C. (1996): Hydrogen positions and thermal expansion in lizardite-1*T* from Elba: a low-temperature study using Rietveld refinement of neutron diffraction data. *Am. Mineral.* **81**, 1111-1116.

GUGGENHEIM, S. & ZHAN, WUDI (1998): Effect of temperature on the structures of lizardite-1*T* and lizardite-2H_1. *Can. Mineral.* **36**, 1587-1594.

HILAIRET, N., DANIEL, I. & REYNARD, B. (2006): P–V equations of state and the relative stabilities of serpentine varieties. *Phys. Chem. Minerals* **33**, 629-637.

MELLINI, M. (1982): The crystal structure of lizardite 1*T*: hydrogen bonds and polytypism. *Am. Mineral.* **67**, 587-598.

MELLINI, M., CRESSEY, G., WICKS, F.J. & CRESSEY, B.A. (2010): The crystal structure of Mg-end member lizardite-1*T* forming polyhedral spheres from the Lizard, Cornwall. *Mineral. Mag.* **74**, 277-284.

MELLINI, M. & VITI, C. (1994): Crystal structure of lizardite-1*T* form Elba, Italy. *Am. Mineral.* **79**, 1194-1198.

MELLINI, M. & ZANAZZI, P.F. (1987): Crystal structures of lizardite-1*T* and lizardite-2H_1 from Coli, Italy. *Am. Mineral.* **72**, 943-948.

MELLINI, M. & ZANAZZI, P.F. (1989): Effects of pressure on the structure of lizardite-1*T*. *Eur. J. Mineral.* **1**, 13-19.

O'HANLEY, D., CHERNOSKY, J.V. & WICKS, F. (1989): The stability of lizardite and chrysotile. *Can. Mineral.* **27**, 483-493.

SHELDRICK, G.M. (1997): SHELX-97, Program for Crystal Structure Determination. University of Göttingen, Göttingen, Germany.

VITI, C. & MELLINI, M. (1997): Contrasting chemical compositions in associated lizardite and chrysotile in veins from Elba, Italy. *Eur. J. Mineral.* **9**, 585-596.

WICKS, F.J. & O'HANLEY, F.C. (1988): Serpentine minerals: structures and petrology. *In* Hydrous Phyllosilicates (Exclusive of Micas) (S.W. Bailey, ed.). *Rev. Mineral.* **19**, 91-159.

WICKS, F.J. & WHITTAKER, E.J.W. (1975): A reappraisal of the structures of the serpentine minerals. *Can. Mineral.* **13**, 227-243.

WUNDER, B. & SCHREYER, W. (1997): Antigorite: high-pressure stability in the system MgO–SiO_2–H_2O (MSH). *Lithos* **41**, 213-227.

Received July 19, 2010, revised manuscript accepted February 14, 2011.

Table 4. Atomic coordinates, isotropic and anisotropic displacement factors (Å^2 x 10^3) of lizardite-1*T* crystals. Estimated standard deviations in parenthesis.

	x/a	y/b	z/c	U_{eq}	U_{11}	U_{22}	U_{33}	U_{23}	U_{13}	U_{12}
Sample Pompeano (3)										
T	1/3	2/3	0.0722(2)	9(1)	6(1)	6(1)	15(1)	0	0	3(1)
M	0.3322(2)	0	0.4532(2)	9(1)	7(1)	7(1)	15(1)	0	0(1)	3(1)
O(1)	1/3	2/3	0.2912(5)	8(1)	8(1)	8(1)	9(1)	0	0	4(1)
O(2)	0.5065(6)	0	-0.0100(5)	14(1)	15(1)	9(1)	16(1)	0	1(1)	4(1)
O(3)	0.6656(5)	0	0.5854(5)	10(1)	10(1)	10(1)	9(1)	0	0(1)	5(1)
O(4)	0	0	0.2984(7)	10(1)	8(1)	8(1)	13(2)	0	0	4(1)
H(3)	0.531(4)	0	0.681(4)	47(9)						
H(4)	0	0	0.149(5)	47(9)						

	x/a	y/b	z/c	U_{eq}	U_{11}	U_{22}	U_{33}	U_{23}	U_{13}	U_{12}
Sample Pompeano (4)										
T	1/3	2/3	0.0718(3)	9(1)	5(1)	5(1)	18(1)	0	0	3(1)
M	0.33245(2)	0	0.4540(3)	10(1)	5(1)	5(1)	19(1)	0	0(1)	3(1)
O(1)	1/3	2/3	0.2911(5)	6(1)	6(1)	6(1)	5(2)	0	0	3(1)
O(2)	0.5064(7)	0	-0.0110(6)	15(1)	18(2)	10(2)	14(1)	0	0(1)	5(1)
O(3)	0.6659(5)	0	0.5850(6)	9(1)	10(1)	10(1)	7(1)	0	0(1)	5(1)
O(4)	0	0	0.2974(7)	7(1)	8(1)	8(1)	7(2)	0	0	4(1)
H(3)	0.846(5)	0	0.592(5)	47(11)						
H(4)	0	0	0.158(4)	47(11)						

	x/a	y/b	z/c	U_{eq}	U_{11}	U_{22}	U_{33}	U_{23}	U_{13}	U_{12}
Sample Sassomorello										
T	1/3	2/3	0.0711(1)	7(1)	6(1)	6(1)	10(1)	0	0	3(1)
M	0.3324(1)	0	0.4528(1)	8(1)	6(1)	6(1)	12(1)	0	0(1)	3(1)
O(1)	1/3	2/3	0.2913(2)	7(1)	7(1)	7(1)	7(1)	0	0	4(1)
O(2)	0.5067(2)	0	-0.0099(2)	12(1)	14(1)	7(1)	12(1)	0	0(1)	4(1)
O(3)	0.6657(1)	0	0.5861(2)	9(1)	9(1)	9(1)	8(1)	0	0(1)	4(1)
O(4)	0	0	0.2983(3)	9(1)	8(1)	8(1)	10(1)	0	0	4(1)
H(3)	0.860(4)	0	0.582(3)	87(9)						
H(4)	0	0	0.154(5)	87(9)						

	x/a	y/b	z/c	U_{eq}	U_{11}	U_{22}	U_{33}	U_{23}	U_{13}	U_{12}
Sample Varana (1)										
T	1/3	2/3	0.0758(2)	7(1)	5(1)	5(1)	11(1)	0	0	3(1)
M	0.3325(2)	0	0.4574(3)	9(1)	5(1)	6(1)	15(1)	0	0(1)	3(1)
O(1)	1/3	2/3	0.2957(6)	7(1)	6(1)	6(1)	8(1)	0	0	3(1)
O(2)	0.5066(6)	0	-0.0063(5)	13(1)	15(1)	9(2)	14(1)	0	0(1)	4(1)
O(3)	0.6657(5)	0	0.5908(5)	9(1)	9(1)	9(1)	7(1)	0	0(1)	5(1)
O(4)	0	0	0.3026(7)	8(1)	7(1)	7(1)	9(2)	0	0	4(1)
H(3)	0.856(3)	0	0.579(4)	42(10)						
H(4)	0	0	0.159(8)	42(10)						

	x/a	y/b	z/c	U_{eq}	U_{11}	U_{22}	U_{33}	U_{23}	U_{13}	U_{12}
Sample Varana (2)										
T	1/3	2/3	0.0768(2)	9(1)	6(1)	6(1)	16(1)	0	0	3(1)
M	0.3324(2)	0	0.4583(3)	9(1)	6(1)	6(1)	15(1)	0	0(1)	3(1)
O(1)	1/3	2/3	0.2963(5)	6(1)	7(1)	7(1)	2(2)	0	0	4(1)
O(2)	0.5071(5)	0	-0.0068(5)	15(1)	17(1)	9(1)	16(2)	0	0(1)	5(1)
O(3)	0.6655(4)	0	0.5882(6)	8(1)	9(1)	9(1)	6(2)	0	0(1)	5(1)
O(4)	0	0	0.3036(7)	7(1)	9(1)	9(1)	4(3)	0	0	5(1)
H(3)	0.868(4)	0	0.582(3)	43(9)						
H(4)	0	0	0.168(6)	43(9)						

	x/a	y/b	z/c	U_{eq}	U_{11}	U_{22}	U_{33}	U_{23}	U_{13}	U_{12}
Sample Santa Scolastica (1)										
T	1/3	2/3	0.0764(3)	7(1)	6(1)	6(1)	8(1)	0	0	3(1)
M	0.3326(4)	0	0.4573(3)	8(1)	5(1)	5(1)	14(1)	0	-1(1)	2(1)
O(1)	1/3	2/3	0.2948(8)	5(1)	5(2)	5(2)	5(3)	0	0	3(1)
O(2)	0.5060(9)	0	-0.0055(8)	15(1)	19(2)	13(2)	12(2)	0	0(2)	7(1)
O(3)	0.6656(9)	0	0.5901(7)	7(1)	10(2)	11(2)	1(2)	0	-1(2)	6(1)
O(4)	0	0	0.3010(9)	6(2)	7(2)	7(2)	3(3)	0	0	4(1)
H(3)	0.834(6)	0	0.644(5)	49(15)						
H(4)	0	0	0.151(5)	49(15)						

Note: U_{eq} is defined as one third of the trace of the ortogonalized U_{ij} tensor. The anisotropic displacement factor exponent takes the form: $exp\ \{-2\pi^2\ [h^2 (a^*)^2 U_{11}+...+2hka^*b^* U_{12}+...]\}$.